Supporting Information

Lam et al. 10.1073/pnas.1313029110

SI Materials and Methods

Cell Culture Studies. ***NHE1 and HVCN1 gene expression levels.*** Total RNA was extracted from freshly harvested cells (Qiagen), treated with DNase I (Promega) and first-strand cDNA was synthesized from 1 μg of total RNA with Oligo (dT) primers (Bio-Rad). *NHE1* and *HVCN1* were amplified with following primers: *NHE1*-forward, ACAGTTCCTGGACCACCTTC; *NHE1*-reverse, TTGAGCTTGTCCTTCCAGTG; *HVCN1*-forward, TCAATGGCATCATCATCTCC; *HVCN1*-reverse, CCGCTCAATTTCTTGTTCCT. Real-time PCR with SYBR green detection (Applied Biosystems) was performed as described (1) using an ABI 7900HT FAST Real-Time PCR System. Dilution series of β-actin were amplified on each plate for all experiments. Transcript levels for all genes from each sample were normalized to β-actin.

Bicarbonate-containing medium. Balanced salt solution (BSS) containing bicarbonate was prepared using solutions in with an initial 12 mM $NaHCO_3$ (in place of 12 mM NaCl), and titrated to pH 7.0 or 7.2 while being bubbled with 5% CO_2/95% air. Final bicarbonate concentrations were 15 mM at pH 7.2 and 9 mM at pH 7.0, as calculated by the Henderson–Hasselbalch relationship: $pH = 6.1 + \log([HCO_3^-]/[H_2CO_3])$. $[H_2CO_3]$ was fixed at 1.14 mM by equilibration with 5% CO_2, and pH was fixed by titration against the 1,4 piperazinediethanesulfonate (PIPES) buffer in the BSS. Studies using these media were performed in a 5% CO_2 incubator to maintain equilibration with CO_2.

Intracellular pH measurement. Neurons were loaded with 1 μM 2′,7′-bis-(2-carboxyethyl)-5-(and-6)-carboxy-fluorescein (BCECF-AM, Molecular Probes) for 15 min before exchange with BSS. Mean fluorescence was recorded from the soma of each neuron in the field of view (15–25 per coverslip). The ratio of fluorescence at 490-nm and 440-nm excitation was determined with a fixed emission wavelength of 535 nm, using 30-ms exposures acquired at 30-s intervals. A pH calibration curve was prepared at the end of each experiment using 20 μM nigericin and 150 mM K^+ solutions buffered with PIPES to the designated pH values (2). H^+ ion values measured in each cell were averaged to generate a mean value for each experiment and condition.

Intracellular calcium measurement. Neurons on glass coverslips were loaded for 30 min with 4 μM fura-4F AM (Molecular Probes) in BSS (3) and washed once with BSS before imaging. Mean fluorescence was recorded from the soma of each neuron in the field of view (15–25 per coverslip). Images were acquired at 1-min intervals with 30-ms exposures, using excitation at both 340 and 380 nm and emission at >510 nm. Calcium changes at each time point were expressed as change in the 340 nm/380 nm signal ratio relative to baseline, and the aggregate data from each experiment was quantified as the mean change recorded over the 35-min observation interval.

Immunofluorescence staining. Formaldehyde-fixed cultures were immunostained as described (4, 5), using rabbit antibody to 4-hydroxynonenal (4HNE; Alpha Diagnostics International, 1:500 dilution) and mouse antibody to microtubule-associated protein 2 (MAP2, Chemicon International, 1:500 dilution). Antibody binding was visualized with Alexa Fluor 488-conjugated anti-mouse IgG or Texas Red 594-conjugated anti-rabbit IgG (Invitrogen) on coverslips mounted onto glass slides using DAPI-containing mounting medium (Vector Laboratories). Negative controls were prepared by omitting the primary antibodies. For quantification of neuronal 4HNE immunostaining, the mean neuronal fluorescence intensity was obtained over the area defined by MAP2 fluorescence. Neurons were analyzed in three randomly chosen optical fields from each of 4–5 coverslips per experiment, with >20 neurons per coverslip, for a total of 40–60 neurons per *n*.

Ethidium imaging. Superoxide was also assessed by evaluating the oxidation of dihydroethidium (DHE) to fluorescent oxidized ethidium species (Eth) (3, 5, 6). Superoxide (or a superoxide metabolite) was confirmed as the reactive oxidant by negation of Eth formation in the studies where NOX2 activity was blocked. DHE (5 μM; Invitrogen) was added to cultures 10 min before the start of the experiment, and maintained throughout. The cultures were photographed at the specified time points with a fluorescence microscope using 510- to 550-nm excitation and > 580-nm emission. For real-time imaging, images of individual neurons were acquired at 1 min intervals (40-ms exposure). Data for each neuron were quantified as mean change in corrected fluorescence over the 35-min observation period, after correction for the rate of change in baseline (pre-NMDA) fluorescence. Each *n* value was the calculated mean response of 15–25 neurons from two coverslips per experiment. For studies using end-point, rather than real-time imaging, Eth fluorescence was measured in three randomly chosen optical fields from each culture well and expressed either as % positive neurons, with positive defined as fluorescence intensity >50% above the mean of control wells, or as the calculated Eth fluorescence area × intensity normalized to cell number. Measurements were obtained in 100–150 neurons in each well, and each experiment was replicated at least three times with independent culture preparations.

Neuronal death. Dead neurons were identified by failure to exclude 0.4% trypan blue dye when assessed 24 h after NMDA treatment. Live and dead neurons were counted in three randomly chosen fields in a minimum of four wells per plate, and results of each experiment were expressed as fold increase in cell death over sister control wells.

In Vivo Studies. ***NMDA injections.*** Adult Black Swiss mice were anesthetized with 2% isoflurane and placed in a stereotaxic frame. The right striatum (anterior-posterior 0.6 mm, medial-lateral 2 mm, and dorsal-ventral 3.5 mm from Bregma) was injected with either saline vehicle, 6 nmol NMDA, 6 nmol 4-isopropyl-3-methylsulfonyl-benzoyl-guanidine-methanesulfonate (HOE), or both NMDA and HOE in 1.2 μL of saline over 5 min. A 1:1 ratio of NMDA to HOE was used instead of the 10:1 ratio used in cell culture because NMDA but not HOE is restricted to the extracellular space. At 30 min or 24 h later, the mice were killed and perfusion-fixed with 4% formaldehyde, and sequential 40-μm cryostat brain sections were taken through the hippocampus and striatum.

Ischemia–reperfusion. Adult $NHE1^{+/-}$ and $NHE1^{+/+}$ mice were subjected to 18 min of bilateral carotid artery occlusion under isoflurane/nitrous oxide anesthesia, as described (7). Core temperature was maintained at 37 ± 0.5 °C by using a homeothermic blanket throughout the surgical procedure. Sham-operated animals received incisions but not artery clamping.

Superoxide formation. Mice were given 1 mg/kg i.p. injections of DHE 15 min before NMDA injection or onset of ischemia, and brains were harvested 30 min after. Brains were sectioned on a cryostat and photographed with a confocal fluorescent microscope at excitation = 510–550 nm and emission >580 nm for detection of oxidized ethidium species (Eth), as described (5, 7). Five sections were analyzed from each brain, taken at 160-μm intervals to span the striatum (for NMDA injections) or hippocampus (for ischemia–reperfusion). For NMDA injections, Eth signal intensity was measured in all nuclei (as defined by DAPI

staining) within 200 μm of the center of the needle track on each section and expressed relative to background (extranuclear) Eth signal. For ischemia–reperfusion studies, mean Eth signal was measured in the stratum radiatum cell layer of hippocampal CA1 and expressed relative to background (extranuclear) Eth signal. Mean values from each section were averaged to generate a single value for each animal.

Superoxide formation in these brain sections was also assessed by immunostaining for 4HNE, as described (5). Sections mounted on slides were boiled in 10 mM sodium citrate (pH 7.0) for 10 min to achieve antigen retrieval before overnight incubation with antibody to 4HNE (1:500; Abcam). Antibody binding was visualized with Alexa Fluor 488-conjugated goat anti-rabbit IgG (1:400; Invitrogen). Immunoreactivity was quantified by determining the mean fluorescence from the CA1 pyramidal cell layer in each slice. Background corrections were done for each image by subtracting the mean fluorescence of an area removed from the pyramidal cell layer, immediately adjacent to stratum oriens. Data from all slices were averaged for each mouse.

Neuronal death. Brains harvested 1 d after NMDA injections were sectioned as above and stained with Fluoro-Jade B method (7), preceded in some cases by NeuN immunostaining (7) to identify neurons. Neuronal death was calculated as the area of Fluor-Jade B staining within 200 μM of the needle track center on each slide, and integrated over the number of sections evaluated (six per mouse).

1. Shen Y, et al. (2011) Mutations in PNKD causing paroxysmal dyskinesia alters protein cleavage and stability. *Hum Mol Genet* 20(12):2322–2332.
2. Thomas JA, Buchsbaum RN, Zimniak A, Racker E (1979) Intracellular pH measurements in Ehrlich ascites tumor cells utilizing spectroscopic probes generated in situ. *Biochemistry* 18(11):2210–2218.
3. Brennan-Minnella AM, Shen Y, El-Benna J, Swanson RA (2013) Phosphoinositide 3-kinase couples NMDA receptors to superoxide release in excitotoxic neuronal death. *Cell Death Dis* 4:e580.
4. Kauppinen TM, Swanson RA (2005) Poly(ADP-ribose) polymerase-1 promotes microglial activation, proliferation, and matrix metalloproteinase-9-mediated neuron death. *J Immunol* 174(4):2288–2296.
5. Brennan AM, et al. (2009) NADPH oxidase is the primary source of superoxide induced by NMDA receptor activation. *Nat Neurosci* 12(7):857–863.
6. Bindokas VP, Jordán J, Lee CC, Miller RJ (1996) Superoxide production in rat hippocampal neurons: Selective imaging with hydroethidine. *J Neurosci* 16(4):1324–1336.
7. Suh SW, et al. (2008) Glucose and NADPH oxidase drive neuronal superoxide formation in stroke. *Ann Neurol* 64(6):654–663.

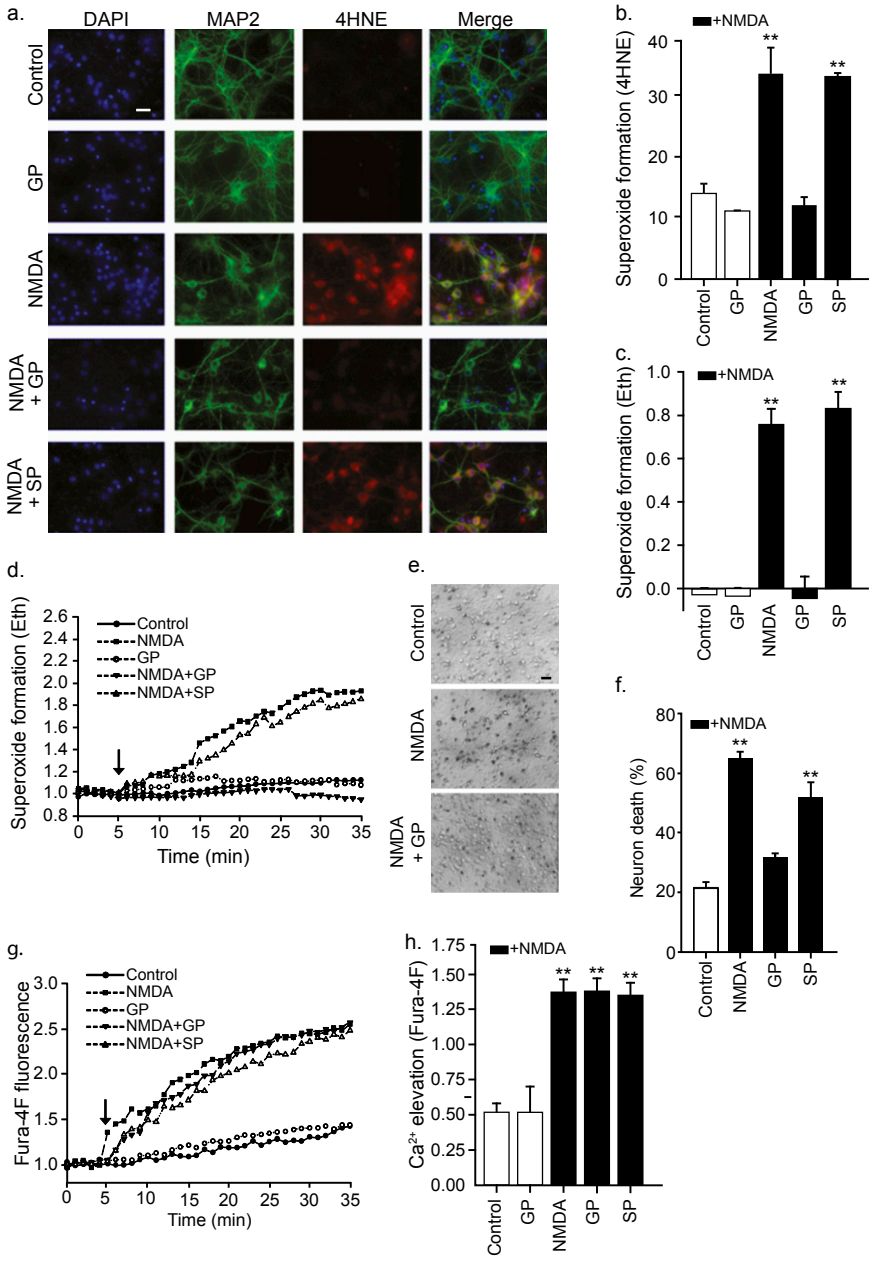

Fig. S1. NADPH oxidase mediates NMDA-induced superoxide formation and cell death. (*A*) Superoxide formation assessed by immunostaining for 4HNE (red) after 20-min incubations in 100 μM NMDA. MAP2 (green) identifies neuronal processes, and DAPI (blue) identifies cell nuclei. The formation of 4HNE is blocked by a tat-conjugated inhibitor of NADPH oxidase (GP, 5 μM), but not by the tat-conjugated scrambled peptide (SP). (Scale bar: 25 μm.) (*B*) Quantified 4HNE immunofluorescence ($n = 4$; $^{**}P < 0.01$ vs. control). (*C*) Representative single-neuron traces of superoxide formation assessed by formation of fluorescent Eth from DHE, conditions as in *A*. Arrow marks addition of NMDA. (*D*) Quantified Eth fluorescence ($n = 4$; $^{**}P < 0.01$ vs. control). (*E*) Neuronal death evaluated by trypan blue staining in phase-contrast photographs of cultures 24 h after treatment as in *A*. (Scale bar: 25 μm.) (*F*) Quantified neuronal death ($n = 3$, $^{**}P < 0.01$ vs. control). (*G*) Representative single-neuron traces showing intracellular calcium elevations as measured by Fura-4F, conditions as in *A*. (*H*) Quantified data show no significant effect of NOX2 inhibition (GP) on NMDA-induced calcium elevation ($n = 4$; $^{**}P < 0.01$ vs. control).

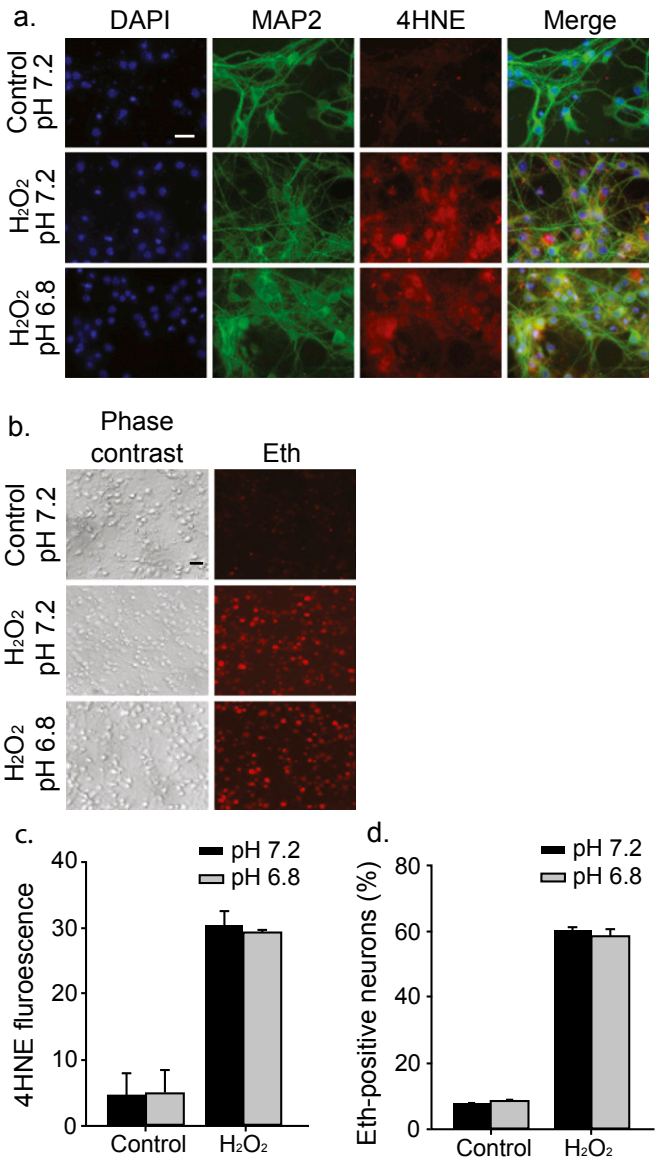

Fig. S2. Acidosis does not suppress direct oxidant-induced formation of 4HNE or Eth. (*A*) Formation of 4HNE (red) after 25-min incubation in 25 μM H_2O_2 at medium pH 7.2 or pH 6.9. MAP2 (green) identifies neuronal processes, and DAPI (blue) identifies cell nuclei. (Scale bar: 25 μm.) (*B*) Formation of fluorescent Eth from DHE, conditions as in *A*. (Scale bar: 25 μm.) (*C* and *D*) Quantified data, $n = 4$.

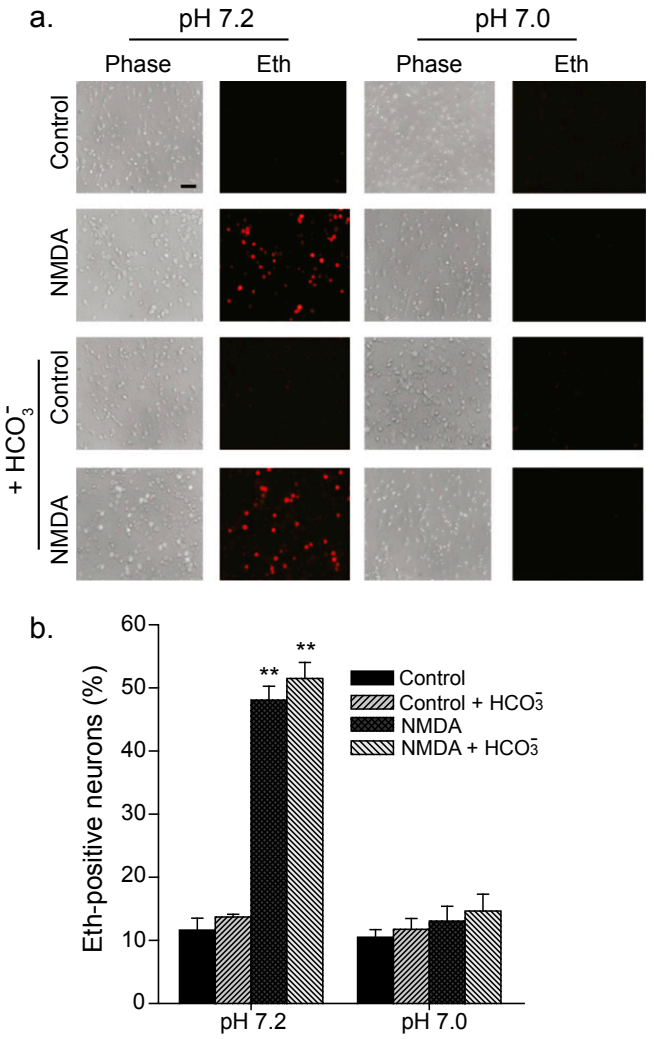

Fig. S3. Acidosis effects on superoxide formation are bicarbonate-independent. Reduction in medium pH from 7.2 to 7.0 blocked NMDA-induced Eth formation in both standard bicarbonate-free medium and in bicarbonate-containing, CO_2-equilibrated medium. Bicarbonate concentrations were 15 mM at pH 7.2 and 9 mM at pH 7.0 (*SI Materials and Methods*). Conditions otherwise as in Fig. 2. (*A*) Formation of fluorescent Eth from DHE after 30 min incubation with 100 μM NMDA. (Scale bar: 25 μm.) (*B*) Quantified results. $n = 4$; $^{**}P < 0.01$ vs. NMDA, pH 7.0.

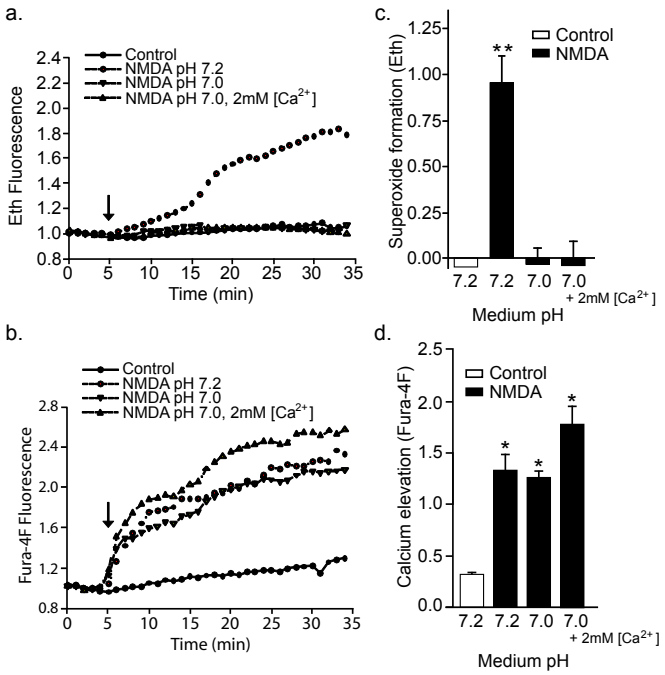

Fig. S4. The effect of acidosis on NMDA-induced superoxide formation can be dissociated from its effects on calcium elevations. (*A* and *B*) Representative simultaneous traces from individual neurons showing the time course of Ca^{2+} elevations (Fura-4F) and superoxide formation (Eth) after addition of 100 μM NMDA. Superoxide formation was prevented at pH 7.0 even with medium Ca^{2+} increased to 2 mM, a value at which the NMDA-induced intracellular Ca^{2+} increase at pH 7.0 exceeds that produced in standard (1.26 mM Ca^{2+} medium at pH 7.2). (*C* and *D*) Quantified data; $n = 3$, $^{*}P < 0.05$ vs. control.

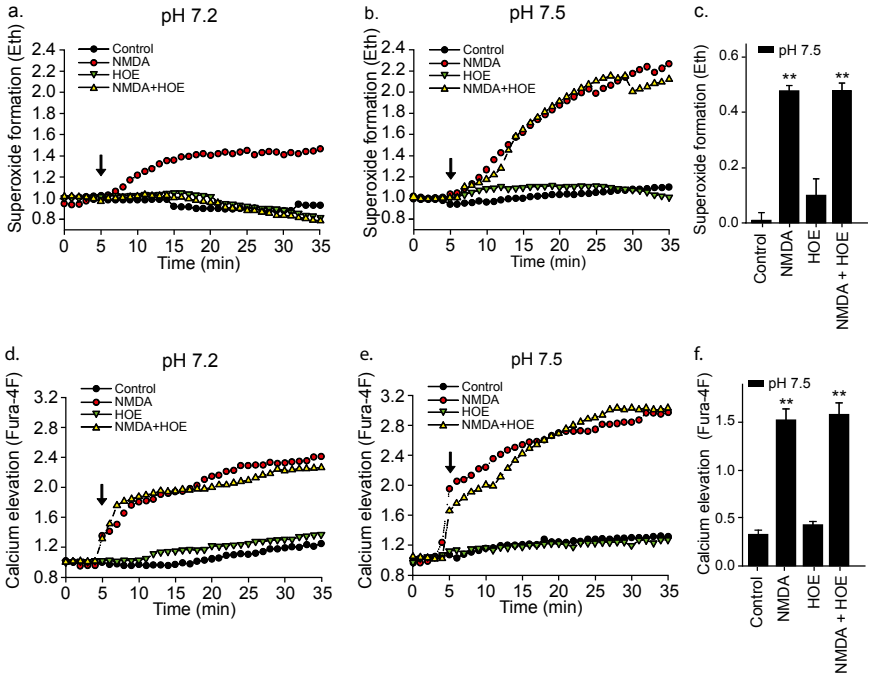

Fig. S5. Effect of HOE on superoxide production is negated by alkalization. (*A* and *B*) Representative single-neuron traces of superoxide formation assessed by formation of fluorescent Eth from DHE, conditions as in Fig. 3. Arrow marks addition of NMDA. Effect of 1 μM HOE is negated at medium pH 7.5 (*C*) Quantified Eth fluorescence ($n = 3$; $^{**}P < 0.01$ vs. control). (*D* and *E*) Representative single-neuron traces showing intracellular calcium elevations as measured by Fura-4F. (*F*) Quantified data show no significant effect of pH or HOE on NMDA-induced calcium elevations ($n = 3$; $^{**}P < 0.01$ vs. control).